

Contents lists available at [ScienceDirect](http://ScienceDirect.com)

# Algal Research

journal homepage: [www.elsevier.com/locate/algal](http://www.elsevier.com/locate/algal)

## Effects of light intensity and carbon dioxide on lipids and fatty acids produced by *Synechocystis* sp. PCC6803 during continuous flow



Sara P. Cuellar-Bermudez<sup>a</sup>, Miguel A. Romero-Ogawa<sup>a</sup>, Raveender Vannela<sup>b</sup>, YenJung Sean Lai<sup>b</sup>, Bruce E. Rittmann<sup>b</sup>, Roberto Parra-Saldivar<sup>a,\*</sup>

<sup>a</sup> Centro de Biotecnología FEMSA, Escuela de Ciencias e Ingeniería, Tecnológico de Monterrey, Monterrey, Nuevo Leon, Mexico

<sup>b</sup> Swette Center for Environmental Biotechnology, The Biodesign Institute, Arizona State University, Tempe, AZ, USA

### ARTICLE INFO

#### Article history:

Received 3 September 2014

Received in revised form 3 July 2015

Accepted 30 July 2015

Available online 22 August 2015

#### Keywords:

*Synechocystis*

Lipids

Fatty acids

Light intensity

CO<sub>2</sub>

pH

### ABSTRACT

We studied the effects of light intensity (LI) and CO<sub>2</sub> supply on pH and total lipid production and fatty acids by *Synechocystis* sp. PCC6803 during continuous-flow operation of a photobioreactor having continuous nutrient supply. The temperature was fixed at 30 °C, and the LI pattern mimicked a day/night light cycle from 0 to 1920 μmol/m<sup>2</sup> s. The CO<sub>2</sub> supply varied from 1 to 5% v/v of total air. The total lipid content increased proportionally to LI, reaching a high content of 14% of dry weight (DW) at the highest LI at 3% CO<sub>2</sub>. In contrast, LI had no significant influence on the total fatty acid content, which was 3.4% ± 0.5% DW, measured as fatty acid methyl esters (FAMES). Palmitic acid (C16:0) was the main fatty acid (52% of FAMES), but γ-linolenic acid (C18:3<sup>n6</sup>) and linoleic acid (C18:2) were significant at 20% and 14% of total FAMES, respectively. Also, α-linolenic acid (C18:3<sup>n3</sup>), oleic acid (C18:1), and palmitoleic acid (C16:1) represented 5%, 4%, and 4% of the total FAMES, respectively. In case of C16:0, its highest content was achieved at LI of 400 to 1500 μmol/m<sup>2</sup> s and pH media values from 7.2 to 8.8 (3% CO<sub>2</sub>). The highest formation of C16:1 and C18:1 (desirable for biodiesel production) occurred with LI up to 600 μmol/m<sup>2</sup> s at pH 9 (3% CO<sub>2</sub>). Stearic acid (C18:0) and linoleic acid (C18:2) contents did not vary with LI or pH, but α-linolenic acid (C18:3<sup>n3</sup>) formation occurred with patterns opposite to C18:3<sup>n6</sup>, C16:0, and C16:1. LI of 400 to 1600 μmol/m<sup>2</sup> s and pH range from 7.7 to 8.7 led to the highest values of C18:3<sup>n6</sup> (0.8% DW), but C18:3<sup>n3</sup> was suppressed by these conditions, supporting a desaturation pathway in *Synechocystis*. These results point to strategies to optimize LI, CO<sub>2</sub>, and pH, to enhance the fatty acid production profile for biofuel production.

© 2015 The Authors. Published by Elsevier B.V. This is an open access article under the CC BY license (<http://creativecommons.org/licenses/by/4.0/>).

### 1. Introduction

Depletion of fossil fuels, increases in oil prices, and the buildup of greenhouse gases have forced countries to investigate renewable energy alternatives to fossil sources. Biofuel production offers opportunities to develop long-term replacements for fossil fuels while also promoting the economies of rural areas [1–3]. Biological CO<sub>2</sub> fixation can be achieved through the photosynthesis of terrestrial plants and microorganisms [4]. Because their CO<sub>2</sub>-fixation efficiency is 10–100 times higher than for plants, eukaryotic algae and cyanobacteria can produce renewable fuel feedstock with much less land, and they do not require arable land [2, 4–6]. Therefore, the mass cultivation of microalgae and cyanobacteria as biomass feedstock for liquid biofuels is being assessed worldwide [7,8].

According to Quintana et al. [9], cyanobacteria have promise for bioenergy generation because they possess higher photosynthesis and growth rates compared to algae. They grow well when provided only

basic nutritional requirements, such as water, CO<sub>2</sub>, mineral salts (especially phosphorus and nitrogen), and light as the only energy source. Moreover, cyanobacteria are amenable to genetic manipulation through the introduction or deletion of genes that allow them to produce more or higher-value products [9–12].

Biodiesel can be produced by transesterification of microalgal lipids, reaction of a simple alcohol (usually methanol) with tri- or diacylglycerides to produce fatty acid methyl esters (FAMES) [13]. FAMES composition determines a biodiesel's oxidative stability and performance properties. Polyunsaturated fatty acids (PUFAs) are susceptible to oxidation, and fully saturated lipids increase the cloud point and viscosity of biodiesel [14]. Therefore, the most desirable lipids are monounsaturated fatty acids (MUFAs) [8]. Microalgal lipids also can be input to a refinery *in lieu* of petroleum feedstock; the fatty acid profile controls fuel quality in a similar way as for biodiesel.

Environmental growth conditions determine the fatty acid profile of lipid in microalgae and cyanobacteria [8,15–20]. Quintana et al. [9] reported that growth conditions affected the fatty acid composition of different cyanobacteria species, Liu et al. [21] noted that the degree of

\* Corresponding author.

E-mail address: [r.parra@itesm.mx](mailto:r.parra@itesm.mx) (R. Parra-Saldivar).

unsaturation in fatty acids increased at lower temperatures, Walsh et al. [22] found that the amount of polyunsaturated fatty acids (PUFAs) decreased in favor of monounsaturated fatty acids at high light intensities, and Gombos et al. [23] found that temperature had a strong impact on the degree of unsaturation of fatty acid groups.

*Synechocystis* sp. PCC6803 was the first photosynthetic organism to have its genome sequenced and is one of the best characterized cyanobacteria in general [11]. It also has been studied for large-scale biomass production based on its growth capability for wide ranges of environmental conditions, such as salt concentration, pH, temperature, and carbon dioxide (CO<sub>2</sub>) level [24–26]. The intracellular lipids in *Synechocystis* are mostly diacylglycerols located in the thylakoid membranes [24,27]. Sheng et al. [16] studied the temperature effect on lipids and fatty acids production in *Synechocystis* sp. PCC6803 and found that the highest fatty acid content in the cells occurred at 30–33 °C. In contrast, 22 °C showed a 20% suppression of lipid synthesis, and 35–40% suppression occurred at 18 °C and 44 °C. Moreover, low temperature (18 and 22 °C) led to higher amounts of PUFA linolenic acid ( $\alpha$ -C18:3 and  $\gamma$ -C18:3).

Cyanobacteria optimize membrane-barrier functions, permeability properties, activities of membrane-bound enzymes, and signaling mechanisms in response to temperature changes [16,28]. Acyl-lipid desaturases introduce double bonds into fatty acids that have been esterified to glycerolipids and are bound to the thylakoid membrane in cyanobacterial cells [29]. *Synechocystis* sp. PCC6803 has been well studied, and its metabolic fatty acid desaturation follows the pathway shown in Fig. 1. Desaturases introduce double bonds at the  $\Delta$ 6,  $\Delta$ 9,  $\Delta$ 12, and  $\Delta$ 15 positions of the fatty acids [30].

In this work, we study how lipid and fatty acid production patterns are controlled by diurnal variations in light intensity, carbon dioxide, and pH for *Synechocystis* sp. PCC6803. These are factors that can vary over wide ranges during the normal day–night conditions of bioenergy generation, and they can be manipulated by engineering measures.

## 2. Materials and methods

### 2.1. Experimental set-up

All experiments were conducted in a vertical, flat-plate photobioreactor (PBR) that consisted of a rectangular body made of polymethyl methacrylate plastic, light panels for irradiation along two sides, and sampling ports with liquid discharging valve along the other two sides. Details of the PBR system are provided by Kim et al. [24,31]. The liquid volume inside the PBR was 14 L. Two mass-flow controllers, connected to a compressed-air tank and a pure-CO<sub>2</sub> tank, regulated the ratio of CO<sub>2</sub> in the air supplied to a gas diffuser installed in the bottom of PBR to achieve good mixing of the reactor contents. Also, an outer-layer water jacket contained water circulating through a water bath (Thermo Scientific Digital Plus) for temperature control. Day–night light intensity (LI) cycling for both sides of the PBR was achieved by using a computer program that created a stepwise pattern imitating the solar irradiation average of a typical day near the autumn equinox in Phoenix, AZ [24,31].

### 2.2. PBR start-up and operating conditions

The PBR was disinfected by washing it once with deionized water contained 0.04% NaOCl. After two rinses with sterile deionized water, the PBR was loaded with 12 L of BG-11 5P medium, which is the standard BG-11 medium with five-fold increased phosphate, or ~28.4 mg P/L [24]. Then, the PBR was inoculated with 2 L of *Synechocystis* sp. PCC6803 culture that had been grown in a glass bottle connected to a filtered-air supply, surrounded by fluorescent lamps that illuminated the vessel continuously, and maintaining at a temperature of ~30 °C. Standard BG-11 medium [32] was used for culture growth. All media were autoclaved before use.

To avoid nutrient depletion and to ensure enough light penetration in the system, the reactor was operated with continuous flow. During

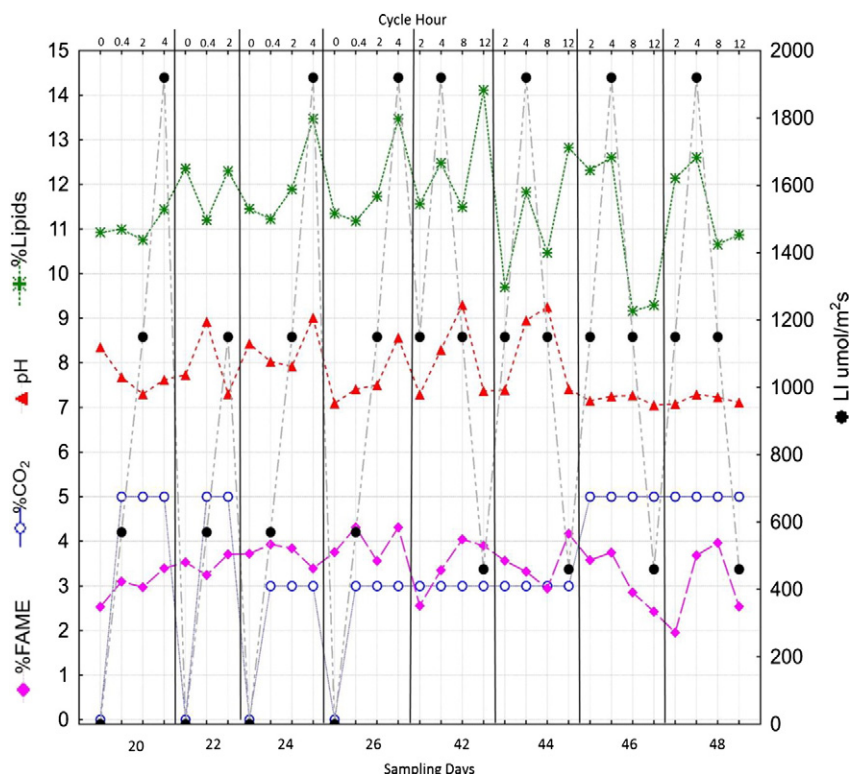


**Fig. 1.** *Synechocystis* sp. PCC6803 pathway of fatty acid desaturation by acyl-lipid desaturases [29,30]. %Lipids, %FAME, and pH values throughout the set of experiments with different LI and %CO<sub>2</sub> inputs for *Synechocystis* sp. PCC6803 in continuous flow. %Lipids and %FAME are percentages of dry weight (DW).

the experiment, air mixed with CO<sub>2</sub> was supplied at the rate of 0.3 L/min to ensure full mixing without liquid overflow. The CO<sub>2</sub> supply was shut off during dark operation, and the light intensity (LI) was held constant at 300 μmol/m<sup>2</sup> s during the first two days of the acclimation phase. This acclimation phase allowed the culture to adapt to higher light intensity and working volume than in the culture bottle of the inoculum. Once the culture reached an OD<sub>730</sub> of 4.4 (~1.2 g DW/L), CO<sub>2</sub>, light cycling, and continuous media flow at 2 mL/min were started.

### 2.3. Sampling and analytical methods

Samples (1-L volume) were taken at the times and LI values shown in Table 1, which also presents the light-intensity pattern for the illuminated time each day. After one day's sampling, the reactor's liquid volume (14 L) was re-established by addition of fresh medium to make up for sampling losses. With sampling every second day, the culture re-grew to OD around 2. The pH and temperature were recorded immediately upon sampling using an Accumet-AB15 pH meter (Fisher Scientific, Waltham, MA) with a glass pH electrode and a glass thermometer. For each sample, 5 mL was filtered through a 0.2-μm polyvinylidene fluoride (PVDF) membrane filter (Whatman, Piscataway, NJ) for NO<sub>3</sub> and PO<sub>4</sub> analysis using an ICS-3000 ion chromatograph (Dionex, Sunnyvale, CA) equipped with anion-exchange column (IonPac AS18, Dionex) [31].

For lipid analysis, cells were harvested and concentrated by centrifugation (Beckman Coulter, Avanti J-26 XPI) at 6000 rpm for 15 min. Later, cell pellets containing solids were frozen for subsequent lyophilization (Labconco FreeZone) at -50 °C under vacuum for 2 days to obtain dry biomass. Total lipid was assayed with 15 mg of dry biomass according to Ryckebosch et al. [33] using chloroform:methanol 1:1 (v/v). The methanol phase was discarded, and the chloroform phase was separated from biomass with a 0.2-μm PTFE membrane filter [34]. Later, the chloroform extracts were moved to a N<sub>2</sub> evaporator (Labconco RapVap N<sub>2</sub>) to remove the chloroform [34]. Finally, dried extracts were weighed to calculate the total lipids extracted.

Fatty acid analysis was performed using a Gas Chromatograph (Shimadzu GC 2010) equipped with a Supelco SP 2380 capillary column (30 m × 0.25 mm × 0.20 μm) coupled with a Flame Ionization Detector (FID) [16]. The first step was trans-esterification, for which 2 ml methanolic HCL (3 N) was added to lipid samples, and the mixture was left overnight in a stoppered tube at 50 °C. Then, fatty acid methyl esters (FAMES) were recovered in 6 mL of hexane for GC-FID samples.

The effects of incident LI and %CO<sub>2</sub> on PCC6803's lipid production, nutrient uptake (dissolved NO<sub>3</sub> and PO<sub>4</sub>), and fatty acid profile were evaluated by regression analysis using one-way ANOVA (One-way ANOVA MODULE, Statistica 12). All samples were considered simultaneously. Comparisons showing a *p* value < 0.05 were considered significantly different. Three-dimensional representations were created using Distance Weighted LS by Statistica Software (Tulsa, OK, USA).

## 3. Results and discussion

### 3.1. Fatty acid profile and ANOVA

Table 2 shows the fatty acids that were detected by GC-FID. Palmitic acid (C16:0) was about 52% of the fatty acid composition, or 1.8% of dry

**Table 1**  
Experiment sampling conditions.

Time (h)	LI (μmol/m <sup>2</sup> s)	%CO <sub>2</sub> (v/v)
0	0	Varied from 1% to 5% for all illuminated times
0.4	570	
2	1150	
4	1920	
8	1050	
12	460	

**Table 2**  
Average fatty acid profile and analysis of variance for correlation to LI and %CO<sub>2</sub>.

Nomenclature	Name	% DW average <sup>a</sup>	%FAMES	<i>p</i> value <sup>b</sup>
C16:0	Palmitic acid	1.77 ± 0.06	51.9	<b>0.031</b>
C16:1	Palmitoleic acid	0.12 ± 0.004	3.6	<b>0.003</b>
C18:0	Stearic acid	0.04 ± 0.001	1.3	0.063
<i>cis</i> -C18:1 <sup>n9</sup>	Oleic acid (ω9)	0.14 ± 0.007	4.2	<b>0.000</b>
<i>cis</i> -C18:2 <sup>n6</sup>	Linoleic acid (ω6)	0.46 ± 0.015	13.7	0.533
C18:3 <sup>n6</sup>	γ-Linolenic (ω6)	0.69 ± 0.035	20.4	<b>0.017</b>
C18:3 <sup>n3</sup>	α-Linolenic (ω3)	0.16 ± 0.026	4.7	<b>0.048</b>
Total FAME		3.41 ± 0.58	100%	0.114
Total lipids		11.6 ± 1.14	-	<b>0.012</b>

<sup>a</sup> Average values produced during continuous flow.

<sup>b</sup> Effects of LI and CO<sub>2</sub> supply are significant at *p* < 0.05, which is indicated with boldface.

weight. γ-Linolenic acid (C18:3<sup>n6</sup>) and linoleic acid (C18:2) were the second and third most common fatty acids, with about 0.69% and 0.46% of dry weight, respectively. This fatty acid composition is similar to what is reported previously by Sheng et al. [16], who also found that C16:0 production was predominant, followed by α-linolenic acid (C18:3<sup>n6</sup>) and C18:2 fatty acids. Table 2 also shows the results of the ANOVA tests for correlations with LI and %CO<sub>2</sub>. Variations in LI and %CO<sub>2</sub> led to significant (*p* < 0.05) variability in %Lipids and production of certain fatty acids: C16:0, C16:1, C18:1, C18:3<sup>n6</sup>, and C18:3<sup>n3</sup>. LI and %CO<sub>2</sub> also significantly affected the pH values (not shown in Table 2, but presented below).

NO<sub>3</sub> and PO<sub>4</sub><sup>-</sup> concentrations were 105 ± 17 mg N/L and 12.1 ± 2.8 mg P/L, respectively. They did not differ significantly among the samples during a day and were high enough that neither nutrient was limiting, the desired experimental situation.

The dominant fatty acids were C16:0 and C18:3<sup>n6</sup> (52% and 20% of total FAME, respectively), but the best biodiesel properties are associated more with MUFAs, such as C16:1 and C18:1, which averaged 3.6% and 4.2% of total FAME, respectively. Thus, it is valuable to identify culture conditions that favor C16:1 and C18:1, versus C16:0 and C18:3<sup>n6</sup>.

Fig. 1 shows the CO<sub>2</sub> supply and LI intensity patterns according to the diurnal light cycle. Also shown are how pH and %Lipids responded to the LI pattern. When the input CO<sub>2</sub> was 3% v/v, pH values increased proportionally with LI so that the highest pH values were obtained at the highest light intensity (1920 μmol/m<sup>2</sup> s), a clear response to photosynthesis activity. Also, when the input CO<sub>2</sub> was 3% v/v, %Lipids increased in parallel to higher LI and then declined as LI decreased. However, higher %CO<sub>2</sub> (5% v/v) did not allow changes in pH, and the effects of LI on %Lipids were muted. In contrast with the trends for pH and %Lipids, but consistent with the ANOVA analysis, %FAME did not show significant trends with LI or %CO<sub>2</sub>.

### 3.2. Trends for pH

Fig. 2, a 3-dimensional plot created by distance weighting, plots trends in pH as a continuous function. Black dots represent the experiment data. Fig. 2 confirms the trends identified by ANOVA (Table 2) and identifies conditions needed to obtain a particular pH value. In general, lower %CO<sub>2</sub> increased the media pH. This trend is expected from the role of CO<sub>2</sub> as an acid. At the highest CO<sub>2</sub> feed level (5%), the pH values were maintained at 7 to 8 without a consistent effect of LI. In contrast, 3% CO<sub>2</sub> led to a systematic trend of increasing pH with LI, with the sharpest increase of LI up to about 500 μmol/m<sup>2</sup> s. For the lowest LI (0–200 μmol/m<sup>2</sup> s), the system pH was around 7, but it reached 9 with LI up at the highest value (1920 μmol/m<sup>2</sup> s), when photosynthetic uptake of CO<sub>2</sub> was greatest. The large range of pH values when the CO<sub>2</sub> level was 3% may have affected %Lipids content, a topic investigated more deeply below. The 3D graph also shows that low CO<sub>2</sub> levels (atmospheric air) could give very high pH values, larger than 10, when the LI was over 500 μmol/m<sup>2</sup> s.

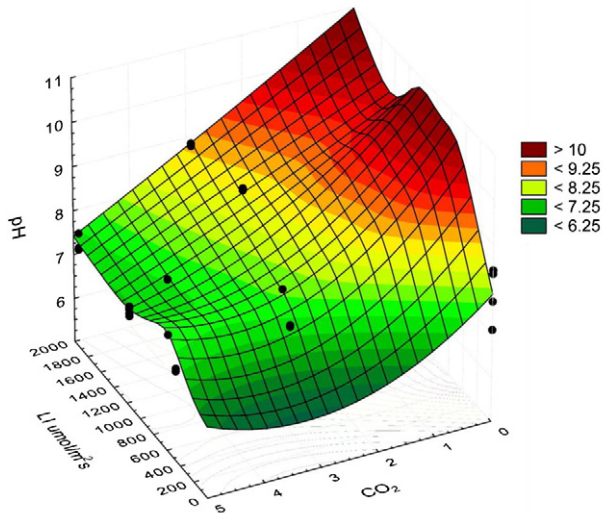


**Fig. 2.** Three-dimensional representation of the effects of %CO<sub>2</sub> and LI on pH. The boundary values of LI and %CO<sub>2</sub> are the ranges of experimental values (Table 1). The black circles are the experimental data.

### 3.3. Trends for lipids

Fig. 3, a 3-dimensional distance-weighting plot, shows the effect of LI on changes in %Lipids and medium pH, and illustrates that most values of %Lipids were around 12% of DW (the largest red area) during the light cycle; this was when media pH values were from 7 to 8.5. For all data, the average %Lipids was 11.6% of DW. That the average value is less than 12% DW reflects the strong decreases for high pH (>9) and low LI (<800 μmol/m<sup>2</sup> s), which together led to much less lipid content, although low LI or high pH alone did not lead to low lipid content. Thus, a combination of limited light availability and restricted CO<sub>2</sub> supply (to give high pH) appeared to cause a low lipid content. In contrast, the highest %Lipids (>14% DW) was associated with high LI (>1600 μmol/m<sup>2</sup> s), but without a strong pH effect.

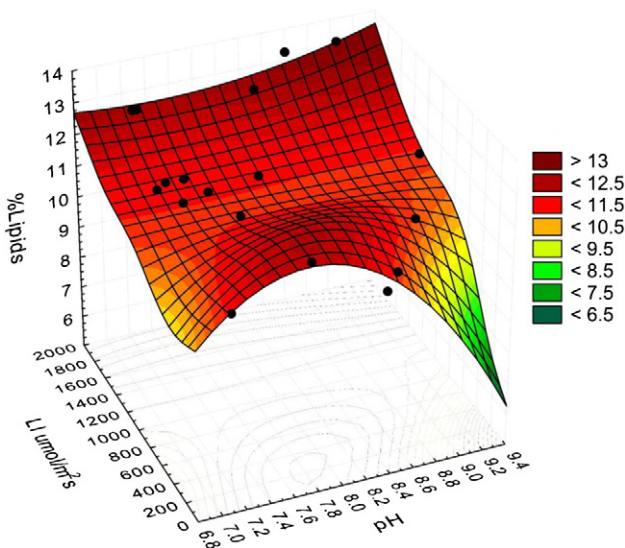


**Fig. 3.** Three-dimensional representation of how changes in LI affected %Lipids (of dry weight) and medium pH.

### 3.4. Trends for fatty acid profiles

Fig. 4, which shows how the fatty acid profile varied with LI, indicates that the total %FAME did not change dramatically or systematically with culture conditions (averaging  $3.41 \pm 0.58\%$  DW). Since %Lipids did change, this relative consistency in %FAME could reflect that other compounds extracted in the lipid fraction, such as pigments or linked protein/carbohydrates [35,36], were what changed in response to LI and pH. While some fatty acids were affected by LI and pH, the major components (C16:0, C18:3<sup>n6</sup>, and C18:2) followed similar patterns. C18:0 was relatively constant at about 1.3% of total FAMES.

Fig. 5 provides a three-dimensional plot for C16:0, the most abundant fatty acid. Previous studies have reported predominant formation of this fatty acid in *Synechocystis* [16,37]. In this experiment, high C16:0 content (2.2% DW) was favored by an LI range of 400 to 1500 μmol/m<sup>2</sup> s and pH values from 7.2 to 8.8. In contrast, low pH (<7.2) during light and high pH (>8.8) led to the lowest content of C16:0 (<1.3% DW). In the case of C16:1 (Fig. S1 Supplementary data), its content was much less than for C16:0. Its highest formation (0.16% DW) occurred at pH from 7.6 to 9, with LI up to 500 μmol/m<sup>2</sup> s, and it followed the same production pattern as C16:0.

According to the ANOVA analysis (Table 2), C18:0 and C18:2 did not show significant differences ( $p$  value < 0.05) with LI or %CO<sub>2</sub>, and they represented only  $0.04\% \pm 0.01$  and  $0.46\% \pm 0.08\%$  DW, respectively. Oleic acid (C18:1) was more important than C18:0 (>0.14% DW). LI values up to 600 μmol/m<sup>2</sup> s and pH up to 9.2 favored its production (>0.16% DW). In addition, pH values from 7 to 7.5 with LI up to 300 μmol/m<sup>2</sup> s also favored C18:1 production (Fig. S2 Supplementary data). In summary, the 3D graphics and ANOVA indicate that *Synechocystis* was able to produce the most C16:1 and C18:1 with LI up to 600 μmol/m<sup>2</sup> s at pH 9. Also, C16:0 production was favored for this condition.

γ-Linolenic acid (C18:3<sup>n6</sup>) (Fig. S3 Supplementary data) and α-linolenic (C18:3<sup>n3</sup>) (Fig. 6) were significant fatty acids (averaging 20 and 5% of total FAMES, respectively) that behaved with opposite patterns. LI of 400 to 1600 μmol/m<sup>2</sup> s and a pH range from 7.7 to 8.7 led to the highest values of C18:3<sup>n6</sup> (0.8% DW), but C18:3<sup>n3</sup> was suppressed within the pH range of 8.1 to 8.7 with LI from 400 to 1500 μmol/m<sup>2</sup> s. Low production of C18:3<sup>n3</sup> at 30–33 °C with BG-11 5P has been reported before [16].

## 4. Discussion

Lipid quantity and composition are key properties that determine biodiesel oxidative stability and performance properties. However, environmental growth conditions determine the lipid quantity and composition (fatty acid profile) in the microorganisms. Cyanobacteria are able to live in a wide range environmental conditions, since they perform oxygenic photosynthesis and respiration at the same time and by the same organelle [38]. Stress factors such as temperature, salinity, pH, heavy metals, and ultraviolet radiation have an effect on cell growth and metabolism. So far, all stresses are reported to show enhanced expression of proteins associated with oxidative damage [39]. However, a number of mechanisms are used to respond to the environmental stressors; these mechanisms involve lipids, amino acids, and enzyme metabolism [40].

When light exposure is too high, microorganism absorbs excess excitation energy causing photo-damage to cells (reduction of acceptor side components of PS II). Also, the photosynthetic reaction center polypeptide D1 is susceptible to damage [41]. In the case of high light adaptation mechanisms in *Synechocystis* sp. PCC6883, the PS I/PSII ratio is about 5, an abundance related to an oxidized plastoquinone pool in the light, minimizing photo damage [38]. He et al. [41] reported that Hli polypeptides (HliA, HliB, HliC) accumulate at high light exposure forming other protein complexes in the thylakoid membrane. Burnap et al. [42] reported that at 3% (v/v) CO<sub>2</sub> and high light intensity

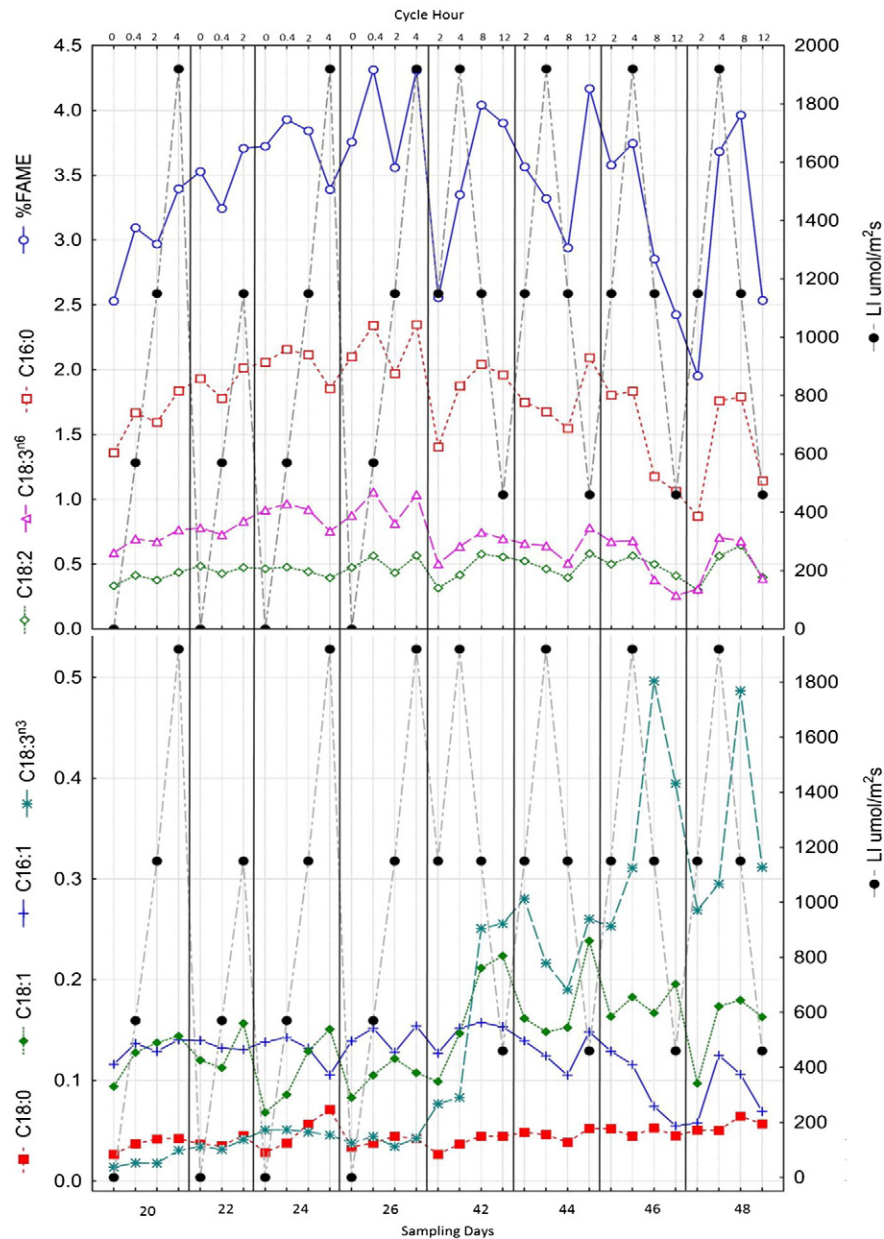


Fig. 4. Fatty acid composition throughout the *Synechocystis* sp. PCC6803 continuous-flow experiments. Results correspond to measurements at the time and LI values shown in Table 1. Values are expressed as % of DW.

(500  $\mu\text{mol}/\text{m}^2 \text{ s}$ ), an increase occurs in the expression of  $\text{CO}_2$  uptake genes *ndhF3* (*sll1732*), *ndhD3* (*sll1733*), *cupA* (*sll1734*), and hypothetical gene (*sll1735*).

According to Srivastava et al. [39], temperature induces changes in membrane fluidity affecting the degree of membrane lipids and protein integrity of membranes. Salinity affects cellular biomolecules by dehydration shell or surface change, also producing reactive oxygen species for oxidative damage. Neutral to alkaline pH is preferred by cyanobacteria; but not many studies about pH-based cellular responses and proteomics exist.

In *Synechocystis*, around 50 ATP-binding cassette (ABC) transport genes have been identified in its genome. These play an important role in nutrient transport and cytoplasmic pH regulation [43]. Summerfield et al. [44] found that pH in the growth medium had a photosystem II (PSII)-specific effect. Also, at elevated pH, cells have higher resistance to oxidative stress. Tahara et al. [43] found that *Slr1045* protein plays a role in the lipid transport system, since acid conditions affected production of phosphatidylglycerol in cell membranes. In

cyanobacteria, another response for pH stress is the increased expression and activity of monovalent cation/proton antiporters, the membrane proteins that maintain intracellular pH [45]. Summerfield and Sherman [45] reported that alkali conditions in *Synechocystis* up-regulate genes encoding two cation/ $\text{H}^+$  antiporters (*NhaS3* and *Mrp*), ATP synthase, and one amino acid deaminase. Other transporters involved in homeostasis include a putative chloride extrusion protein (*Slr0753*), a mechanosensitive channel acting as calcium channel, and a hexose/proton symporter with other ABC transporter subunits [45].

Although we did not perform proteomic analysis, the noted adaptation mechanisms (gene level) reported for cyanobacteria (especially *Synechocystis*) point out the value of future proteomic research when several factors, such as light intensity, pH and temperature, are combined. We interpret the effects of external pH (media pH) and light intensity according to changes in fatty acid profiles.

Intracellular pH is affected by external pH. A unit increment of pH in the medium results in a 10% increment in pH values in the cytosol and thylakoid lumen; however, pHs within these two compartments are

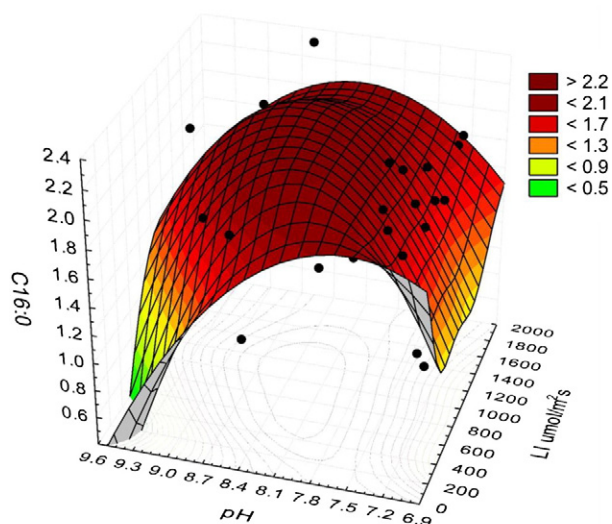


Fig. 5. Palmitic acid (C16:0) production results, expressed as % of DW.

different, the pH of the thylakoid lumen being ~2 pH units lower than the pH on the cytosol [45]. These changes, for example, have an effect on the intracellular inorganic carbon concentration ( $\text{CO}_2/\text{HCO}_3^-$ ) affecting the carboxylase activity of Rubisco.

In this article, the changes of medium pH were analyzed in terms of fatty acid metabolism. In *Synechocystis*, the intracellular lipids are mostly located in the thylakoid membranes [24,27], where pH is different than the medium pH. It is the intracellular pH that affects the metabolic pathway for fatty acid saturation/desaturation. Although we cannot link the fatty acid changes to the intracellular pH values, we are able to identify enzymatic metabolic pathways depending on external pH (nutrients,  $\text{CO}_2$  and light). For example, the shift from  $\alpha$ -linolenic and  $\gamma$ -linolenic acid confirms a desaturation pathway in *Synechocystis*, and the  $\Delta 12$  desaturase seems to have been expressed at pH values from 7.7 to 8.7, leading to C18:3<sup>n6</sup> formation. In contrast, a  $\Delta 15$  desaturase for C18:3<sup>n3</sup> formation seems to have been expressed at pH values lower than 7.5 and higher than 9.

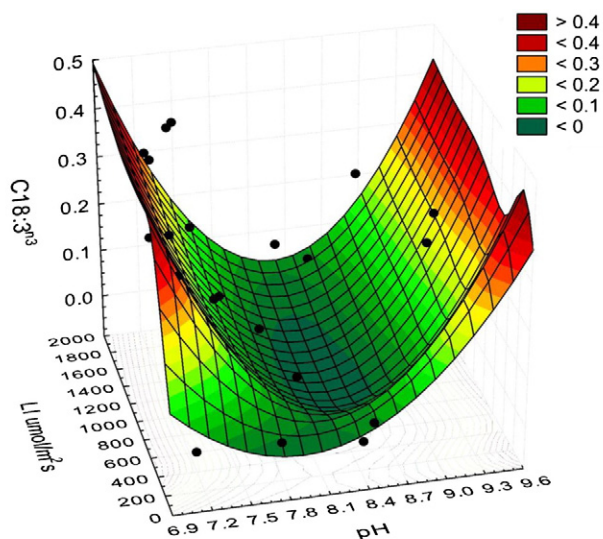


Fig. 6.  $\alpha$ -Linolenic acid (C18:3<sup>n3</sup>) production results, expressed as % of DW.

## 5. Conclusions

Comparisons within the day/night light cycle with temperature controlled at 30 °C showed that the lipid fraction produced by *Synechocystis* sp. PCC6803 was affected by LI and pH media. In general, %Lipids increased in proportional to LI and was greatest for pH of 9 (3%  $\text{CO}_2$ ). In contrast, %FAME was relatively constant, which probably means that other components extracted as part of total lipids changed also in response to LI and pH. C16:0 was the main fatty acid (averaging ~52%), and it was favored by an LI range of 400 to 1500  $\mu\text{mol}/\text{m}^2 \text{ s}$  and pH values from 7.2 to 8.8 (3%  $\text{CO}_2$ ). Other significant components of the fatty acid profile also were affected by LI and pH. C18:3<sup>n6</sup> and C18:2 were the second and third most important fatty acids produced by *Synechocystis*, representing, respectively, ~20% and 14% of total FAMES on average. C18:3<sup>n6</sup> responded to LI and pH similarly to C16:0, but C18:2 was not altered by LI and pH. Also significant were C18:3<sup>n3</sup>, C18:1, and C16:1, being ~5%, 4%, and 4% of total FAMES, respectively.  $\alpha$ -Linolenic acid (C18:3<sup>n3</sup>) formation occurred with patterns opposite to C18:3<sup>n6</sup>, C16:0, and C16:1. While LI of 400 to 1600  $\mu\text{mol}/\text{m}^2 \text{ s}$  and a pH range from 7.7 to 8.7 led to the highest values of C18:3<sup>n6</sup> (0.8% DW), C18:3<sup>n3</sup> was suppressed with these conditions, supporting a desaturation pathway in *Synechocystis*. For the best biodiesel properties, MUFAs such as C16:1 and C18:1 are preferred. During the experiments, C16:1 and C18:1 became greater fractions with LI up to 600  $\mu\text{mol}/\text{m}^2 \text{ s}$  at pH 9 (3%  $\text{CO}_2$ ). According to our results, a 3% v/v of  $\text{CO}_2$  allowed high lipid production and a favorable fatty acid profile in continuous flow growth of *Synechocystis* sp. PCC6803. Therefore, culture conditions, particularly LI,  $\text{CO}_2$  and pH, should be controllable to favor production of these fatty acids.

## Acknowledgments

CONACyT (343023) (Mexican National Science and Technology Council) support and assistance provided to Sara Paulina Cuellar-Bermudez during this investigation at Arizona State University are gratefully acknowledged.

## Appendix A. Supplementary data

Supplementary data to this article can be found online at <http://dx.doi.org/10.1016/j.algal.2015.07.018>.

## References

- [1] J.R. Benemann, Utilization of carbon dioxide from fossil fuel-burning power plants with biological systems, *Energy Convers. Manag.* 34 (1993) 999–1004.
- [2] L. Brennan, P. Owende, Biofuels from microalgae—a review of technologies for production, processing, and extractions of biofuels and co-products, *Renew. Sust. Energ. Rev.* 14 (2010) 557–577, <http://dx.doi.org/10.1016/j.rser.2009.10.009>.
- [3] A. Demirbas, M.F. Demirbas, *Algae energy: algae as a new source of biodiesel*, Green Ener, Springer, 2010.
- [4] S.H. Ho, C.Y. Chen, D.J. Lee, J.S. Chang, Perspectives on microalgal  $\text{CO}_2$ -emission mitigation systems — a review, *Biotechnol. Adv.* 29 (2011) 189–198.
- [5] Y. Chisti, Biodiesel from microalgae, 25 (2007) 294–306, <http://dx.doi.org/10.1016/j.biotechadv.2007.02.001>.
- [6] S.P. Cuellar-Bermudez, J.S. García-Perez, B.E. Rittmann, R. Parra-Saldivar, Photosynthetic bioenergy utilizing  $\text{CO}_2$ : an approach on flue gases utilization for third generation biofuels, *J. Clean. Prod.* 98 (2015) 53–65, <http://dx.doi.org/10.1016/j.jclepro.2014.03.034>.
- [7] B.E. Rittmann, Opportunities for renewable bioenergy using microorganisms, *Biotechnol. Bioeng.* 100 (2008) 203–212, <http://dx.doi.org/10.1002/bit.21875>.
- [8] G.O. James, C.H. Hocart, W. Hillier, G.D. Price, M.A. Djordjevic, Temperature modulation of fatty acid profiles for biofuel production in nitrogen deprived *Chlamydomonas reinhardtii*, *Bioresour. Technol.* 127 (2013) 441–447, <http://dx.doi.org/10.1016/j.biortech.2012.09.090>.
- [9] N. Quintana, F. Van der Kooy, M.D. Van de Rhee, G.P. Voshol, R. Verpoorte, Renewable energy from Cyanobacteria: energy production optimization by metabolic pathway engineering, *Appl. Microbiol. Biotechnol.* 91 (2011) 471–490, <http://dx.doi.org/10.1007/s00253-011-3394-0>.
- [10] V. Gupta, S.K. Ratha, A. Sood, V. Chaudhary, R. Prasanna, New insights into the biodiversity and applications of cyanobacteria (blue-green algae)—prospects and challenges, *Algal Res.* 2 (2013) 79–97, <http://dx.doi.org/10.1016/j.algal.2013.01.006>.

- [11] L. Rosgaard, A.J. de Porcellinis, J.H. Jacobsen, N.-U. Frigaard, Y. Sakuragi, Bioengineering of carbon fixation, biofuels, and biochemicals in cyanobacteria and plants, *J. Biotechnol.* 162 (2012) 134–147, <http://dx.doi.org/10.1016/j.jbiotec.2012.05.006>.
- [12] X. Lu, A perspective: photosynthetic production of fatty acid-based biofuels in genetically engineered cyanobacteria, *Biotechnol. Adv.* 28 (2010) 742–746, <http://dx.doi.org/10.1016/j.biotechadv.2010.05.021>.
- [13] I.M.P. Machado, S. Atsumi, Cyanobacterial biofuel production, *J. Biotechnol.* 162 (2012) 50–56, <http://dx.doi.org/10.1016/j.jbiotec.2012.03.005>.
- [14] G. Knothe, Fuel properties of highly polyunsaturated fatty acid methyl esters. prediction of fuel properties of algal biodiesel, *Energy Fuel* 26 (2012) 5265–5273, <http://dx.doi.org/10.1021/ef300700v>.
- [15] A. Richmond (Ed.), *Handbook of Microalgal Culture*, Blackwell Publishing Ltd, Oxford, UK, 2004 <http://dx.doi.org/10.1002/9780470995280>.
- [16] J. Sheng, H.W. Kim, J.P. Badalamenti, C. Zhou, S. Sridharakrishnan, R. Krajmalnik-Brown, et al., Effects of temperature shifts on growth rate and lipid characteristics of *Synechocystis* sp. PCC6803 in a bench-top photobioreactor, *Bioresour. Technol.* 102 (2011) 11218–11225, <http://dx.doi.org/10.1016/j.biortech.2011.09.083>.
- [17] C. Yeesang, B. Cheirsilp, Effect of nitrogen, salt, and iron content in the growth medium and light intensity on lipid production by microalgae isolated from freshwater sources in Thailand, *Bioresour. Technol.* 102 (2011) 3034–3040, <http://dx.doi.org/10.1016/j.biortech.2010.10.013>.
- [18] I.A. Guschina, J.L. Harwood, Lipids and lipid metabolism in eukaryotic algae, *Prog. Lipid Res.* 45 (2006) 160–186, <http://dx.doi.org/10.1016/j.plipres.2006.01.001>.
- [19] I.C. de Loura, J.P. Dubacq, J.C. Thomas, The effects of nitrogen deficiency on pigments and lipids of cyanobacteria, *Plant Physiol.* 83 (1987) 838–843.
- [20] S.E. Karatay, G. Dönmez, Microbial oil production from thermophile cyanobacteria for biodiesel production, *Appl. Energy* 88 (2011) 3632–3635, <http://dx.doi.org/10.1016/j.apenergy.2011.04.010>.
- [21] X.-J. Liu, Y. Jiang, F. Chen, Fatty acid profile of the edible filamentous cyanobacterium *Nostoc flagelliforme* at different temperatures and developmental stages in liquid suspension culture, *Process Biochem.* 40 (2005) 371–377, <http://dx.doi.org/10.1016/j.procbio.2004.01.018>.
- [22] K. Walsh, G.J. Jones, R. Hugh Dunstan, Effect of irradiance on fatty acid, carotenoid, total protein composition and growth of *Microcystis aeruginosa*, *Phytochemistry* 44 (1997) 817–824, [http://dx.doi.org/10.1016/S0031-9422\(96\)00573-0](http://dx.doi.org/10.1016/S0031-9422(96)00573-0).
- [23] Z. Gombos, H. Wada, N. Murata, Unsaturation of fatty acids in membrane lipids enhances tolerance of the cyanobacterium *Synechocystis* PCC6803 to low-temperature photoinhibition, *Proc. Natl. Acad. Sci. U. S. A.* 89 (1992) 9959–9963 (<http://www.pubmedcentral.nih.gov/articlerender.fcgi?artid=50253&tool=pmcentrez&rendertype=abstract> (accessed February 06, 2014)).
- [24] H.W. Kim, R. Vannela, C. Zhou, B.E. Rittmann, Nutrient acquisition and limitation for the photoautotrophic growth of *Synechocystis* sp. PCC6803 as a renewable biomass source, *Biotechnol. Bioeng.* 108 (2011) 277–285, <http://dx.doi.org/10.1002/bit.22928>.
- [25] T. Ogawa, A. Kaplan, Inorganic carbon acquisition systems in cyanobacteria, *Photosynth. Res.* 77 (2003) 105–115, <http://dx.doi.org/10.1023/A:1025865500026>.
- [26] Y. Kanesaki, I. Suzuki, S.I. Allakhverdiev, K. Mikami, N. Murata, Salt stress and hyperosmotic stress regulate the expression of different sets of genes in *Synechocystis* sp. PCC 6803, *Biochem. Biophys. Res. Commun.* 290 (2002) 339–348, <http://dx.doi.org/10.1006/bbrc.2001.6201>.
- [27] J. Sheng, R. Vannela, B.E. Rittmann, Disruption of *Synechocystis* PCC 6803 for lipid extraction, *Water Sci. Technol.* 65 (2012) 567–573, <http://dx.doi.org/10.2166/wst.2012.879>.
- [28] D. Chapman, Phase transitions and fluidity characteristics of lipids and cell membranes, *Q. Rev. Biophys.* 8 (2009) 185, <http://dx.doi.org/10.1017/S0033583500001797>.
- [29] N. Murata, H. Wada, Acyl-lipid desaturases and their importance in the tolerance and acclimatization to cold of cyanobacteria, *Biochem. J.* 308 (Pt 1) (1995) 1–8.
- [30] D.A. Los, N. Murata, Structure and expression of fatty acid desaturases, *Biochim. Biophys. Acta Lipids Lipid Metab.* 1394 (1998) 3–15, [http://dx.doi.org/10.1016/S0005-2760\(98\)00091-5](http://dx.doi.org/10.1016/S0005-2760(98)00091-5).
- [31] H.W. Kim, R. Vannela, C. Zhou, C. Harto, B.E. Rittmann, Photoautotrophic nutrient utilization and limitation during semi-continuous growth of *Synechocystis* sp. PCC6803, *Biotechnol. Bioeng.* 106 (2010) 553–563, <http://dx.doi.org/10.1002/bit.22724>.
- [32] R. Rippka, J. Deruelles, J.B. Waterbury, M. Herdman, R.Y. Stanier, Generic assignments, strain histories and properties of pure cultures of cyanobacteria, *J. Gen. Microbiol.* 111 (1979) 1–61, <http://dx.doi.org/10.1099/00221287-111-1-1>.
- [33] E. Ryckebosch, K. Muylaert, I. Foubert, Optimization of an analytical procedure for extraction of lipids from microalgae, *J. Am. Oil Chem. Soc.* 89 (2011) 189–198.
- [34] J. Sheng, R. Vannela, B.E. Rittmann, Evaluation of methods to extract and quantify lipids from *Synechocystis* PCC 6803, *Bioresour. Technol.* 102 (2011) 1697–1703, <http://dx.doi.org/10.1016/j.biortech.2010.08.007>.
- [35] R. Halim, M.K. Danquah, P.A. Webley, Extraction of oil from microalgae for biodiesel production: a review, *Biotechnol. Adv.* 30 (2012) 709–732, <http://dx.doi.org/10.1016/j.biotechadv.2012.01.001>.
- [36] D.L. Palmquist, T.C. Jenkins, Challenges with fats and fatty acid methods, *J. Anim. Sci.* 81 (2003) 3250–3254.
- [37] T. Cai, X. Ge, S.Y. Park, Y. Li, Comparison of *Synechocystis* sp. PCC6803 and *Nannochloropsis salina* for lipid production using artificial seawater and nutrients from anaerobic digestion effluent, *Bioresour. Technol.* 144 (2013) 255–260, <http://dx.doi.org/10.1016/j.biortech.2013.06.101>.
- [38] *Encyclopedia of Life Sciences*, John Wiley & Sons, Ltd, Chichester, UK, 2001.
- [39] S. Rai, S. Pandey, A.K. Shrivastava, P.K. Singh, C. Agrawal, L.C. Rai, Understanding the mechanisms of abiotic stress management in cyanobacteria with special reference to proteomics, *Stress Biology of Cyanobacteria, Molecular Mechanisms to Cellular Responses*, CRC Press, Boca Raton, USA, 2013.
- [40] S.C. Singh, S.P. Rajeshwar, D.P. Häder, Role of lipids and fatty acids in stress tolerance in cyanobacteria, *Acta Protozool.* 41 (2002) 297–308.
- [41] Q. He, N. Dolganov, O. Bjorkman, A.R. Grossman, The high light-inducible polypeptides in *Synechocystis* PCC6803. Expression and function in high light, *J. Biol. Chem.* 276 (2001) 306–314, <http://dx.doi.org/10.1074/jbc.M008686200>.
- [42] R.L. Burnap, R. Nambudiri, S. Holland, Regulation of the carbon-concentrating mechanism in the cyanobacterium *Synechocystis* sp. PCC6803 in response to changing light intensity and inorganic carbon availability, *Photosynth. Res.* 118 (2013) 115–124, <http://dx.doi.org/10.1007/s1120-013-9912-4>.
- [43] H. Tahara, J. Uchiyama, T. Yoshihara, K. Matsumoto, H. Ohta, Role of Slr1045 in environmental stress tolerance and lipid transport in the cyanobacterium *Synechocystis* sp. PCC6803, *Biochim. Biophys. Acta* 1817 (2012) 1360–1366, <http://dx.doi.org/10.1016/j.bbabi.2012.02.035>.
- [44] T.C. Summerfield, T.S. Crawford, R.D. Young, J.P.S. Chua, R.L. Macdonald, L.A. Sherman, et al., Environmental pH affects photoautotrophic growth of *Synechocystis* sp. PCC 6803 strains carrying mutations in the luminal proteins of PSII, *Plant Cell Physiol.* 54 (2013) 859–874, <http://dx.doi.org/10.1093/pcp/pct036>.
- [45] T.C. Summerfield, L.A. Sherman, Global transcriptional response of the alkali-tolerant cyanobacterium *Synechocystis* sp. strain PCC 6803 to a pH 10 environment, *Appl. Environ. Microbiol.* 74 (2008) 5276–5284, <http://dx.doi.org/10.1128/AEM.00883-08>.